

A. Ait Said, K. Bey, H. Mzad*

Laboratory of Industrial Mechanics, Badji Mokhtar University of Annaba, P.O. Box 12, DZ-23000, Algeria

*Corresponding author. E-mail: h_mzad@yahoo.fr

Received (Otrzymano) 27.12.2020

COUPLED EFFECT OF LOAD RATIO AND FREQUENCY ON MECHANICAL FATIGUE BEHAVIOUR OF PRECAST ALUMINIUM/ARAMID FIBRE COMPOSITE

Dynamic tests with different load ratios and frequencies provide designers with the necessary information to evaluate the longevity of different structures as well as minimize weight due to a possibly smaller factor of safety. The influence of loading frequency on the fatigue behaviour of an aluminium composite material (ACP) with an aramid honeycomb core was studied. The mechanical behaviour was assessed by three-point static bending tests, followed by cyclic flexural fatigue tests employing the fabricated sandwich samples, with loading frequencies of 5, 7.5 and 10 Hz. The experimental results were presented on a single graph in order to highlight the different behaviours for the adopted frequencies. Indeed, the tests allowed the authors to determine the different cycle number values necessary to achieve resistance losses of 10 and 25%, respectively. The experiments were carried out for the same loading level of 80% of the maximum force, which is taken as equal to the elastic limit in order to avoid the field of plastic deformations.

Keywords: composite sample, experimental tests, loading frequency, cycle number, flexural fatigue, test-end criterion

INTRODUCTION

Composite sandwich structures are special types of composite materials that are produced by inserting a thick, lightweight core between two thin, stiff and strong polymer composite face-sheets. Also, an adhesive material is used to join the face-sheet to the core. Since the thickness of the structure increases, its bending load bearing capacity is also enhanced.

Sandwich panels are an example of a sandwich structured composite: the strength and lightness of this technology makes it popular and widespread. Its versatility means that the panels have many applications and come in many forms: the core and skin materials can vary widely and the core may be a honeycomb or a solid filling [1].

Recently, studies on the fabrication and mechanical behaviors of newly-manufactured sandwich structures with a hexagon honeycomb core have been conducted [2-4]. Parametric studies are performed considering different stiffener configurations, panel thicknesses and materials in composite sandwich panels.

The fields of application, properties and performance of composite sandwich structures have been examined and compared in many research works in the last few decades [5-9]. The creep, static and fatigue characteristics of polyurethane foam-cored sandwich structures and end-grain balsa with hexagonal honeycombs constructed of aluminium or aramid paper and PVC

cores were scrutinized. Square-cell honeycomb was also considered in predicting the free-vibration response of infinitely long and rectangular sandwich panels. Moreover, the tribological and permeability properties of carbon-copper composites and synthetic gypsum, paraffin and polymers were experimentally investigated.

Bousfia et al. [10], formulated a hybrid procedure in order to predict the damage of a laminate composed of UD FRP laminate under random loading. The technique is based on a stiffness degradation model (SDM) combined with an energy approach taking into account the effect of the load ratio. A coupling algorithm was developed to survey the damage progress of the composite laminate and consequently predict its damage rupture.

Test frequency exerts a considerable influence on the dynamic mechanical behaviour of composite materials. The effect of test frequency on the fatigue behaviour of a carbon fibre/epoxy matrix composite is examined in [11]. The monitored dynamic mechanical property responses reflect a strong dependence of the angle ply specimen fatigue response on the test frequency.

The very high cycle fatigue behaviour of a glass fibre-reinforced laminate and carbon fibre-reinforced polymers was tested at six different load levels. A special high-frequency four-point bending test rig was set

up, in a frequency range between 50 and 80 Hz and a stress ratio between 0.29 and 0.49, to circumvent common problems such as specimen heating [12, 13]. Load cycle numbers of up to 10^8 and 10^9 were reached within acceptable testing times.

The influence of the loading frequency on the fatigue behaviour of a coir fibre-reinforced polypropylene composite was considered in [14]. The mechanical behaviour was assessed through monotonic tensile and flexural tests, followed by cyclic bending fatigue tests employing new specimen geometry, with loading frequencies ranging from 5 to 35 Hz.

The experimental results of tension-tension stress-controlled fatigue tests, performed on an advanced sheet moulding compound (A-SMC), are presented in [15]. It was shown that the coupled effect of the loading amplitude and the frequency affects the nature of the overall fatigue response, which can be governed by the accumulation of damage mechanisms and/or by self-heating.

Industry needs products with high a dynamic strength to weight ratio. Usually static mechanical properties are presented in handbooks and adapted for dynamic loading conditions with a factor of safety. Unfortunately, the use of such a method does not provide enough understanding about how long the specific structure will work under certain conditions. The proposed work is an experimental study on the mechanical fatigue behaviour of an aramid/aluminium composite panel with a honeycomb core under three-point bending stress. The influence of the loading frequency on this behaviour, using four specimens, is investigated through static bending and fatigue tests within a defined range of excitation frequencies and loading levels.

SPECIFICATIONS AND TESTS CONDITIONS

The main concept of the sandwich structure is that exterior surfaces transfer loads caused by bending (flexural load and compression), while the core transfers load caused by shearing. Accordingly, the work mode of the sandwich panel described macroscopically can be rightly compared to tasks performed by an I-beam.

There are various options for designing a composite sandwich panel (Fig. 1). Any variation in the facesheet, core type and overall geometry will have a great impact on the general structural properties.

The studied sandwich panel, with aluminium skins and an aramid honeycomb core, was fabricated in the laboratory. The designed samples were obtained from thin sheets 175 μm thick, partially glued and stacked, which thereafter underwent expansion. The core/skin connection was ensured by gluing using epoxy adhesive film.

Test pieces were cut according to the "L" direction of the sandwich panel cells. Their dimensions (Fig. 2) were defined according to the AFNOR NF 54-606 stan-

dard. Width b of the specimen was set at 25 mm to meet the standard requirements. The exact dimensions of the panel were: skin thickness $t_f = 1$ mm, core $c = 8$ mm thick, and the structure thickness $h = 10$ mm. Total length L of the test piece was 200 mm. The cells or alveoli of the sandwich composite of the nida-core were shaped like a regular hexagon with an inscribed diameter of 6.4 mm and 148 kg/m^3 density (Fig. 3). A honeycomb shaped structure provides a material with minimal density and relative high out-of-plane compression properties and out-of-plane shear properties (Table 1).

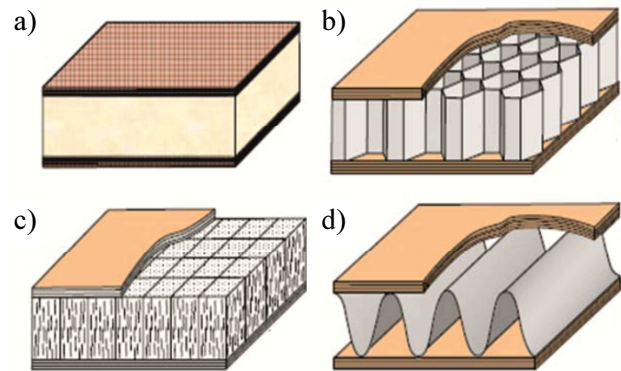


Fig. 1. Composite structures types: a) foam core, b) balsa core, c) honeycomb core, d) corrugated core

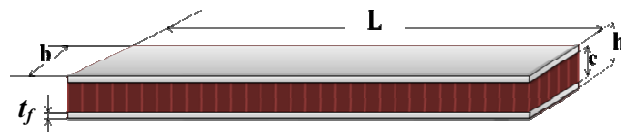
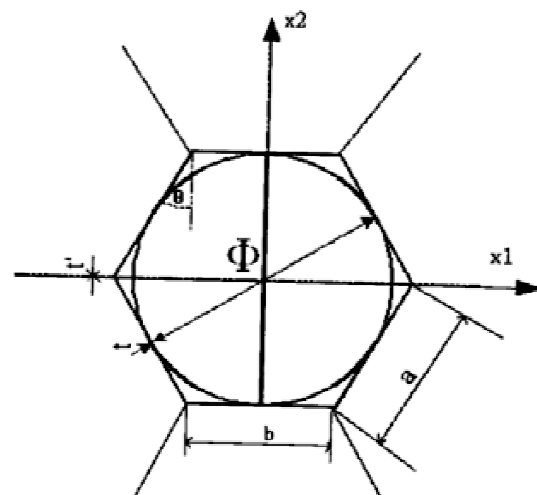


Fig. 2. Sandwich specimen dimensions



Characteristic	Value
Cell angle	$\theta = 30^\circ$
Cell diameter	$\Phi = 6.4 \text{ mm}$
Inclined wall length	$a = 3.695 \text{ mm}$
Horizontal wall length	$b = 3.695 \text{ mm}$
Central wall thickness	$t' = 400 \mu\text{m}$
Inclined wall thickness	$t = 175 \mu\text{m}$

Fig. 3. Alveolus dimensions

TABLE 1. Mechanical properties of composite panel

Material property		Value
Aramid core	Cell size	3.2 mm
	Density	148 kg/m ³
	Shear resistance (<i>L</i> direction)	3.5 MPa
	Shear modulus (<i>L</i> direction)	130 MPa
	Compressive strength (<i>L</i> direction)	15.5 MPa
Aluminium Skins	Young's modulus	70000
	Tear resistance	270 MPa
	Tensile strength	370 MPa
	Elongation to break	13%
	Poisson's ratio	0.33



Fig. 4. Static bending test machine

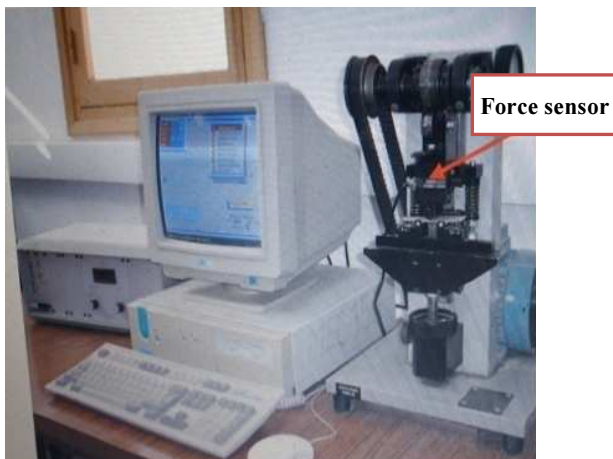


Fig. 5. Bending fatigue testing device (Epsiflex machine)

Static bending tests (Fig. 4):

- Number of trials: 4
- Speed: 5 mm/min
- Temperature: 27°C
- AF 54-606 compliant inter-support: $L = 120$ mm

Flexural fatigue tests (Fig. 5):

- Corrugated sinusoidal loading
- Loading frequency of 5 Hz
- Ratio $L/h = 12$
- Load ratio fixed at $R = f_{min}/f_{max} = 0.2$

EXPERIMENT RESULTS

Static tests

Experimental bending tests under monotonic load ratio were performed in order to plot the resistance loss graphs.

Composite design in the case of fatigue loading is usually characterized by an S-N curve, from which one may obtain a Wöhler curve. This later can be presented as a curve giving the value of the cyclic stress amplitude. Unfortunately, the software used by the available testing machine uses only forces in the ordinate axis instead of stresses. Nevertheless, we believe that the shape of the obtained curve is very significant and similar to the usually presented S-N (Fig. 6).

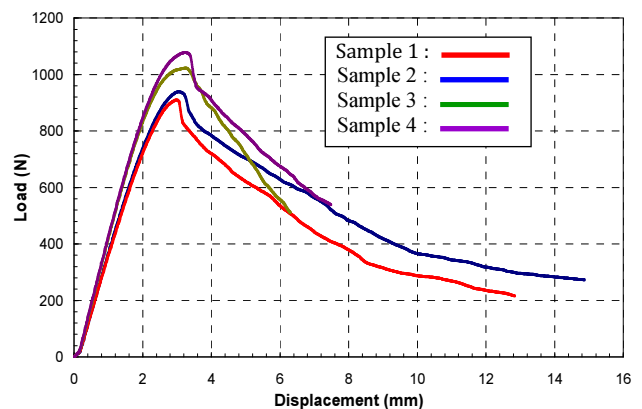


Fig. 6. Force-displacement curves

There are three zones of deformation:

- A linear zone corresponding to elastic deformation up to a limit value (≈ 760 N) corresponding to an arrow $f \approx 2$ mm.
- A non-linear area corresponding to plastic deformation up to the maximum value (≈ 960 N).
- A non-linear zone corresponding to damage by plastic deformation with a decreasing appearance without reaching a final rupture.

Endurance tests

Four tests, illustrated in Figure 7, were performed for three loading levels:

- First load level of 90% with initial loading force $F_o = 0.9 F_{max} = 648$ N,
- Second load level of 80% with initial loading force $F_o = 0.8 F_{max} = 576$ N,
- Third load level of 70% with initial loading force $F_o = 0.7 F_{max} = 504$ N.

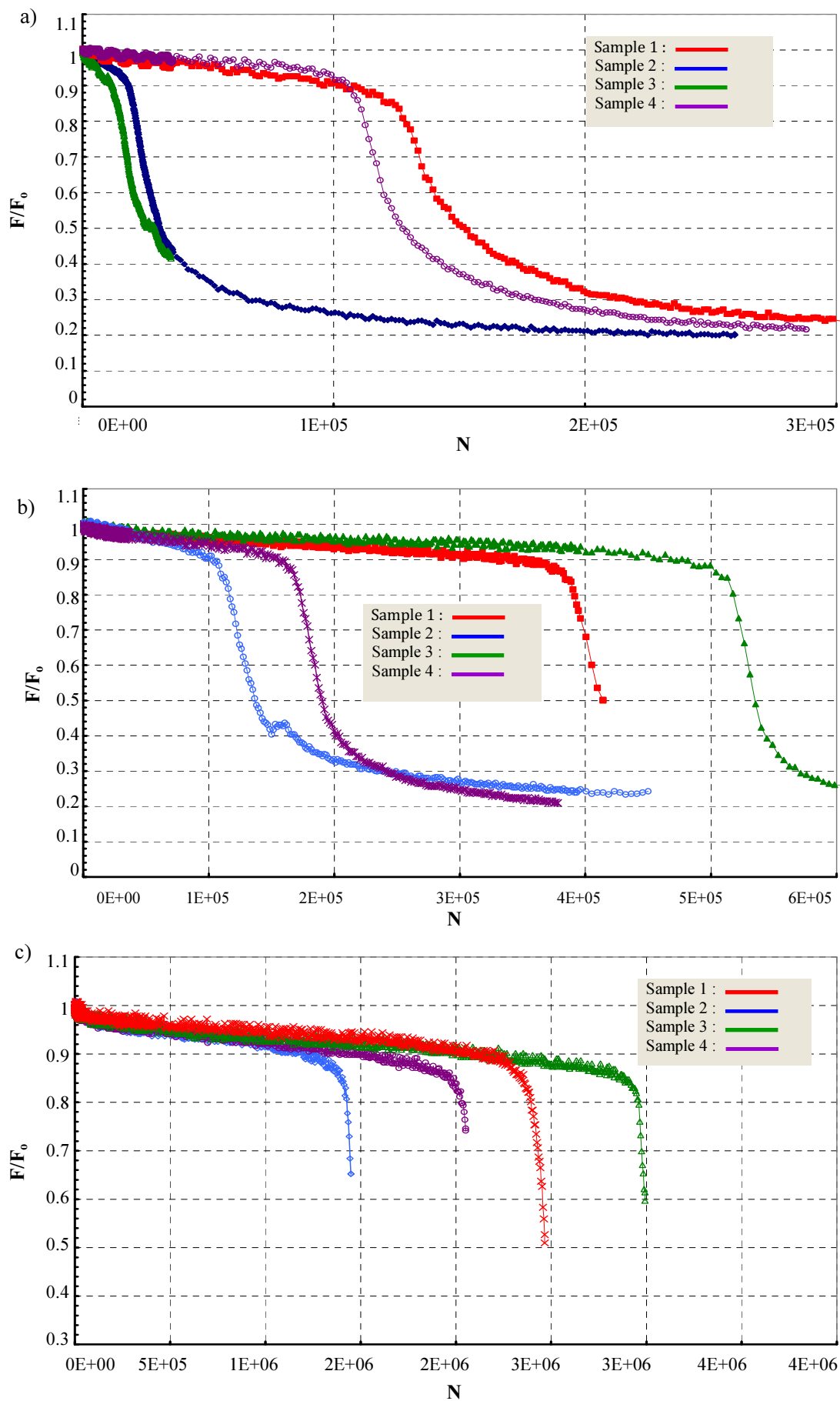


Fig. 7. Resistance loss curves: a) 90% load, b) 80% load, c) 70% load

Influence of excitation frequency

The loading frequency was varied for the intermediate level (80%) by setting it respectively at 5, 7.5 and 10 Hz (Fig. 8).

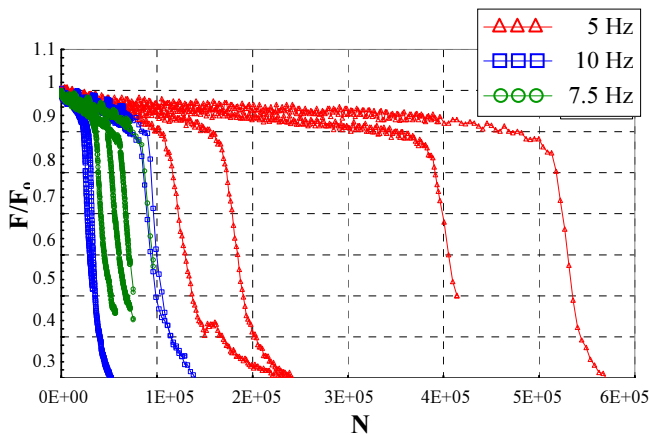


Fig. 8. Resistance loss curves

Interpretation of experimental curves

In what follows, N_{10} and N_{25} are the numbers of cycles necessary for the material to lose, respectively, 10 and 25% of its resistance, i.e. when the F/F_0 ratio reaches, respectively, the values 0.9 and 0.75. Important characteristics, set out below, concerning the number of cycles characterizing the test end criteria can be noticed on the resistance loss curves (Fig. 8).

Test end criterion 90%

The necessary number of cycles to obtain a resistance loss of 10% (N_{10}) is given by the following ranges:

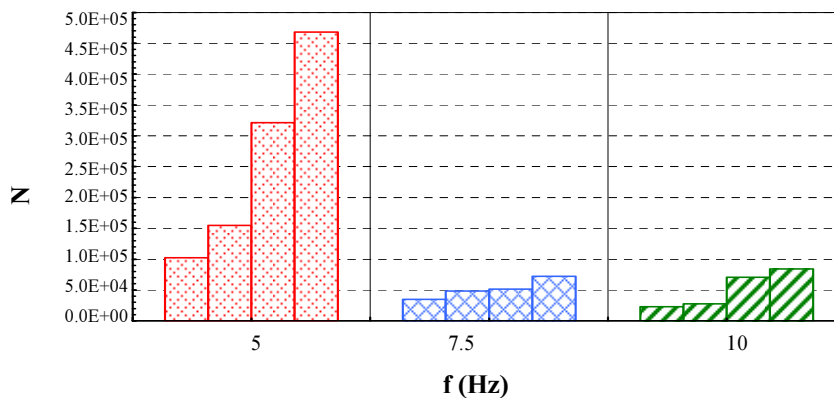
- $[10^5, 4.7 \times 10^5]$ for specimens subjected to fatigue tests at the frequency of 5 Hz.
- $[3.5 \times 10^4, 7.2 \times 10^4]$ for specimens subjected to fatigue tests at the frequency of 7.5 Hz.
- $[2.3 \times 10^4, 8.4 \times 10^4]$ for specimens subjected to fatigue tests at the frequency of 10 Hz.

TEST-END CRITERION OF 90%, R = 0.2

f = 5 Hz		Specimen 1	Specimen 2	Specimen 3	Specimen 4
Load level 80%	N	102050	154550	321050	468050
	Log N	11.53321817	11.94827295	12.67935215	13.05633041
	F/F ₀	0.9	0.9	0.9	0.9
	Max deflection amplitude (mm)	1.57	1.57	1.57	1.57

f = 7.5 Hz		Specimen 1	Specimen 2	Specimen 3	Specimen 4
Load level 80%	N	35100	48200	51400	72100
	Log N	10.4659564	10.7831143	10.8473935	11.1858093
	F/F ₀	0.9	0.9	0.9	0.9
	Max deflection amplitude (mm)	1.57	1.57	1.57	1.57

f = 10 Hz		Specimen 1	Specimen 2	Specimen 3	Specimen 4
Load level 80%	N	23100	27600	70700	84100
	Log N	10.0475879	10.2255711	11.1662009	11.3397618
	F/F ₀	0.9	0.9	0.9	0.9
	Max deflection amplitude (mm)	1.57	1.57	1.57	1.57



Test-end criterion: 90%

Test end criterion 75%

The necessary number of cycles to obtain a resistance loss of 25% (N_{25}) is given by the following ranges:

- $[1.2 \times 10^5, 5.2 \times 10^5]$ for specimens subjected to fatigue tests at the frequency of 5 Hz.
- $[4 \times 10^4, 9 \times 10^4]$ for specimens subjected to fatigue tests at the frequency of 7.5 Hz.

- $[2.6 \times 10^4, 9.7 \times 10^4]$ for specimens subjected to fatigue tests at the frequency of 10 Hz.

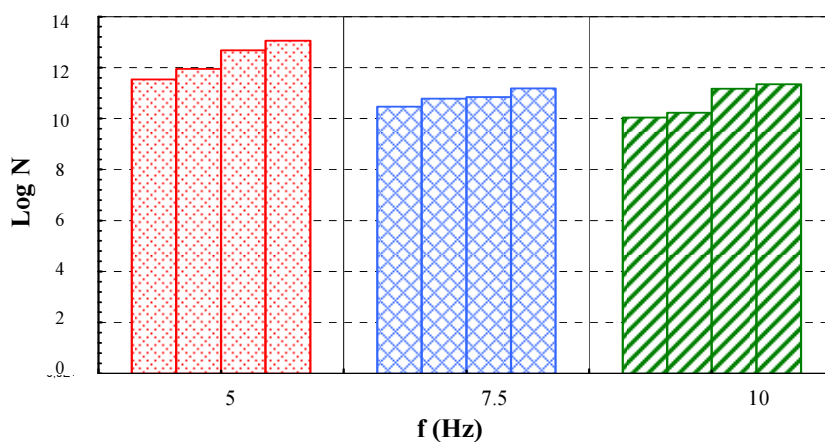
The material behaviour in the three-point cyclic bending fatigue test for the three loading frequencies, represented by the resistance loss curves in Figure 8, is presented in detail by means of explicit tables and histograms. Considering the previous test end criteria, each batch of 4 specimens is cyclically loaded with the same frequency.

TEST-END CRITERION OF 75%, R = 0.2

f = 5 Hz		Specimen 1	Specimen 2	Specimen 3	Specimen 4
Load level 80%	N	120050	175550	394550	522050
	Log N	11.6956636	12.07567918	12.88550115	13.16551865
	F/F ₀	0.75	0.75	0.75	0.75
	Max deflection amplitude (mm)	1.57	1.57	1.57	1.57

f = 7,5 Hz		Specimen 1	Specimen 2	Specimen 3	Specimen 4
Load level 80%	N	39700	54000	65800	90100
	Log N	10.5891065	10.8967393	11.0943751	11.4086754
	F/F ₀	0.75	0.75	0.75	0.75
	Max deflection amplitude (mm)	1.57	1.57	1.57	1.57

f = 10 Hz		Specimen 1	Specimen 2	Specimen 3	Specimen 4
Load level 80%	N	26000	31300	87100	97100
	Log N	10.1658518	10.3513734	11.3748122	11.4834967
	F/F ₀	0.75	0.75	0.75	0.75
	Max deflection amplitude (mm)	1.57	1.57	1.57	1.57



Test-end criterion: 75%

Damage of studied material

For the fracture mechanics analyses, after the fatigue and bending testing (Figs. 9 and 10), a light microscope, together with image analysis was used. The equipment consists of three parts: a light microscope, a macro observation system and a PC with image analysis software.

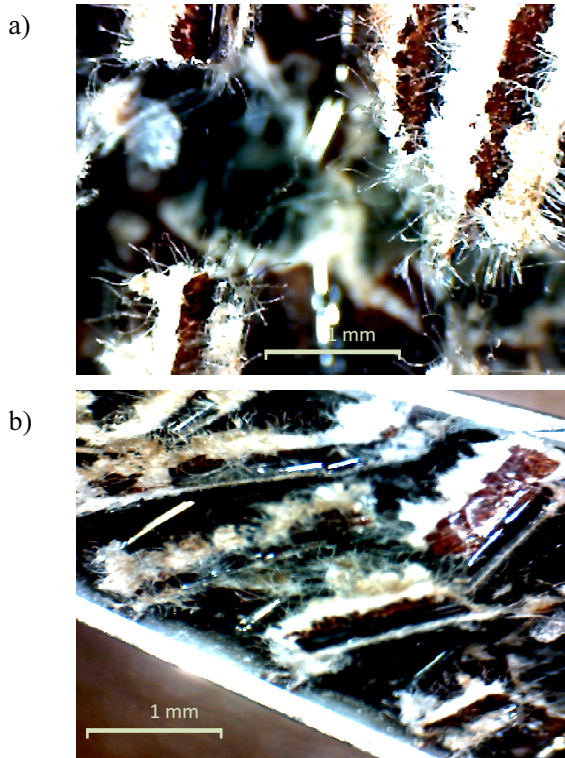


Fig. 9. Shearing of core walls: a) in static bending, b) in fatigue bending

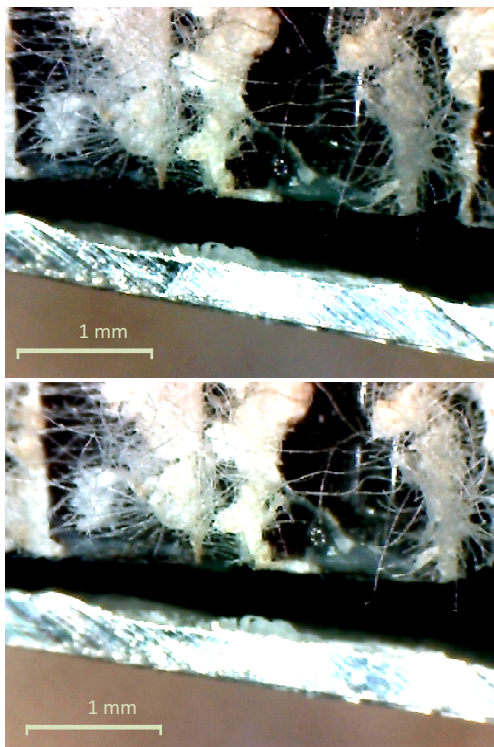


Fig. 10. Disbonding of core: a) in static bending, b) in fatigue bending



Fig. 11. Indentation of skins

Brief comments on results

Microscopic analysis provides even better understanding of the different damage modes involved in various loading conditions. Observation by a light microscope, after static and cyclic flexion, allowed the different modes of damage to be examined. The magnifications (Figs. 9-11) show indentation of the skins and detachment and/or shearing of the honeycomb core, leading to the deterioration of the samples.

In terms of damage, we can perceive during static bending:

- significant indentation of the skins (Fig. 11),
- cracking of the core, causing rupture of the cells,
- separation of the core (Fig. 10a).

In cyclic stress:

- slight indentation of the skins following plastic deformation (Fig. 11),
- buckling of the cells causing their shearing (Fig. 9b),
- separation of the core (Fig. 10b).

CONCLUSIONS

The experiments carried out on the mechanical fatigue behaviour of an aluminium/aramid composite panel with an alveoli core in three-point bending revealed that high strain rates during monotonic loading lead to higher flexural strength. Moreover, high loading frequencies in cyclic bending tests reduce the fatigue life of the sandwich panel, and the criterion for test ending is reached more rapidly. Fractographic examination showed that one of the reasons for the reduced fatigue life under higher loading frequencies might be related

to the increased heat generation by hysteresis, leading to a fatigue damage mechanism.

The outcomes that emerge from this study show that sandwich panels with a honeycomb core have mechanical characteristics comparable to homogeneous materials. The loss of resistance becomes significant after a large number of cycles. However, a delay in the material resistance loss was noticed for moderate cyclic loadings at average frequencies (from 1 to 10 Hz). The skins and then the core are respectively damaged, leading to failure of the specimens, without a premature buckling effect.

Finally, it can be concluded that the life expectancy of Al/Aramid sandwich composites is strongly influenced by a coupled effect between the loading force-ratio and frequency. The test-end criterion is determined depending on the excitation frequency. Thus, the results encourage the development of good practices regarding test frequencies in order to be able to understand the mechanical effects and provide relevant data for structural integrity assessments.

REFERENCES

- [1] Allen H.G., Analysis and Design of Structural Sandwich Panels, 1st edition. Pergamon, Oxford 1969.
- [2] Kiyak B., Kaman M.O., Mechanical properties of new-manufactured sandwich composite having carbon fiber core, *Journal of Composite Materials* 2019, 53(22), 3093-3109.
- [3] Wei X., Li D., Xiong J., Fabrication and mechanical behaviors of an all-composite sandwich structure with a hexagon honeycomb core based on the tailor-folding approach, *Composites Science and Technology* 2019, 184, 107878.
- [4] El-Fasih M.Y., Kueh A.B.H., Ibrahim M.H.W., Failure behavior of sandwich honeycomb composite beam containing crack at the skin, *PLoS ONE*, 15(2), e0227895, 2020.
- [5] Chevalier J.L., Creep, fatigue and fire resistance of chemical tank sandwich cores, *Journal of Reinforced Plastics and Composites* 1994, 13(3), 250-261.
- [6] Burton W.S., Noor A.K., Assessment of continuum models for sandwich panel honeycomb cores, *Computer Methods in Applied Mechanics and Engineering* 1997, 145, 341-360.
- [7] Kim J.H., Lee Y.S., Park B.J., Kim D.H., Evaluation of durability and strength of stitched foam-cored sandwich structures, *Composite Structures* 1999, 47, 543-550.
- [8] Matsagar V.A., Comparative performance of composite sandwich panels and non-composite panels under blast loading, *Materials and Structures* 2016, 49, 611-629.
- [9] Powala K., Heim D., Paraffin permeability of synthetic gypsum binders modified by individual polymers, *Latvian Journal of Physics and Technical Sciences* 2019, 6, 47-56.
- [10] Bousfia M., Aboussaleh M., Ouhbi B., Damage prediction hybrid procedure for FRP laminates subjected to random loads, *Composites Theory and Practice* 2020, 20(2), 67-71.
- [11] Barron V., Buggy M., Mckenna N.H., Frequency effects on the fatigue behaviour on carbon fibre reinforced polymer laminates, *Journal of Materials Science* 2001, 36, 1755-1761.
- [12] Adam T.J., Horst P., Experimental investigation of the very high cycle fatigue of GFRP [90/0]_s cross-ply specimens subjected to high-frequency four-point bending, *Composites Science and Technology* 2014, 101, 62-70.
- [13] Backe D., Balle F., Eifler D., Fatigue testing of CFRP in the very high cycle fatigue (VHCF) regime at ultrasonic frequencies, *Composites Science and Technology* 2015, 106, 93-99.
- [14] de Moraes D.V.O., Magnabosco R., Donato G.H.B., Bettini S.H.P., Antunes M.C., Influence of loading frequency on the fatigue behavior of coir fibre reinforced PP composite, *Polymer Testing* 2015, 41, 184-190.
- [15] Shirinbayan M., Fitoussi J., Meraghni F., Surowiec B., Laribi M., Tcharkhtchi A., Coupled effect of loading frequency and amplitude on the fatigue behavior of advanced sheet molding compound (A-SMC), *Journal of Reinforced Plastics and Composites* 2017, 36(4), 271-282.